Calcif Tissue Int (1990) 46:20–27

Calcified Tissue International
© 1990 Springer-Verlag New York Inc.

Formation of Carbonate-Apatite Crystals After Implantation of Calcium Phosphate Ceramics

G. Daculsi,[1] R. Z. LeGeros,[2] M. Heughebaert,[3] and I. Barbieux[1]

[1]U225 INSERM, Unite de Recherche sur les Tissus Calcifies, [2]UFR Odontologie, Nantes, France; [2]New York University College of Dentistry, New York, New York, USA; and [3]Laboratoire de Physico-chimie des Solides, Ecole de Chimie, Toulouse, France

Summary. The aims of this study were (1) to determine at the crystal level, the nonspecific biological fate of different types of calcium phosphate (Ca-P) ceramics after implantation in various sites (osseous and nonosseous) in animals and (2) to investigate the crystallographic association of newly formed apatitic crystals with the Ca-P ceramics.

Noncommercial Ca-P ceramics identified by X-ray diffraction as calcium hydroxylapatite (HA), beta-tricalcium phosphate (β-TCP), and biphasic calcium phosphates (BCP) (consisting of β-TCP/HA = 40/60) were implanted under the skin in connective tissue, in femoral lamellar cortical bone, articular spine bone, and cortical mandibular and mastoidal bones of animals (mice, rabbits, beagle dogs) for 3 weeks to 11 months. In humans, HA or β-TCP granules were used to fill periodontal pockets, and biopsies of the implanted materials were recovered after 2 and 12 months.

Results of this study demonstrated the following: (1) the presence of needle-like microcrystals (new crystals) associated with the Ca-P ceramic macrocrystals in the microporous regions of the implants regardless of the sites of implantation (osseous or nonosseous), type of Ca-P ceramics (HA, β-TCP, BCP), type of species used (mice, rabbits, dogs, humans), or duration of implantation; (2) decrease in the area occupied by the ceramic crystals and the subsequent filling of the spaces between the ceramic crystals by the new crystals; (3) these new crystals were identified as apatite by electron diffraction and as carbonate-apatite by infrared absorption spectroscopy; (4) high resolution transmission electron microscopy (Hr TEM) revealed one family of apatite lattice fringes in the new crystals in continuity with the lattice planes of the HA of β-TCP ceramic crystals; (5) Hr TEM also demonstrated the presence of linear dislocations at the junction of the new apatite crystals and ceramic crystals.

It is suggested that the formation of the CO_3 apatite crystals associated with the implanted Ca-P ceramic is due to dissolution/precipitation and secondary nucleation involving an epitatic growing process and not to an osteogenic property of the ceramic.

Key words: Calcium phosphate — Ceramic — Biomaterial — Biocompatibility — Mineralization — Apatite.

Send reprint requests to Dr. R. Z. LeGeros, New York University College of Dentistry, 345 East 24th Street, New York, NY 10010, USA.

Commercial and noncommercial calcium phosphate (Ca-P) ceramics described as hydroxylapatite (HA) and tricalcium phosphate (TCP) have been extensively explored as bone substitutes in bone repair [1–5]. Some of the commercial Ca-P ceramics have been characterized by X-ray diffraction as calcium HA ($Ca_{10}(PO_4)_6(OH)_2$), or beta-tricalcium phosphate (-TCP) ($Ca_3(PO_4)_2$), or a mixture of HA and β-TCP referred to as biphasic calcium phosphates (BCP) [2, 5, 6].

Recent studies by Daculsi et al. [7–9] and others [10, 11] demonstrated the presence of needle-like crystals in the vicinity of the large crystals of HA ceramics after implantation in osseous sites. The presence of these crystals were interpreted by some investigators to show "osteogenic" properties of the HA ceramic [10, 11]. Crystals have also been observed on the surface of "nonresorbable" HA

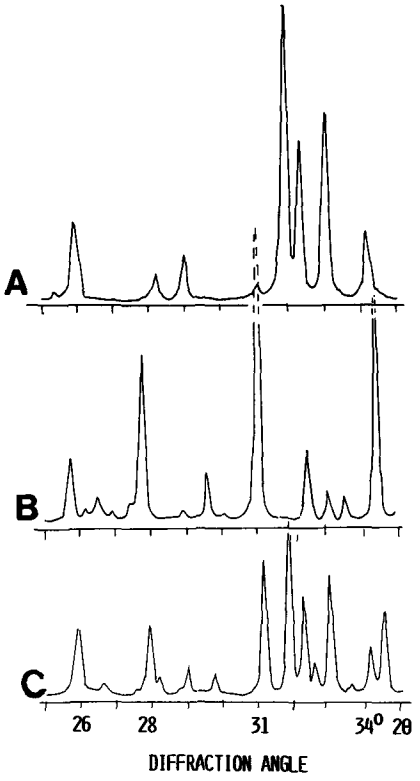

Fig. 1. X-ray diffraction patterns of noncommercial calcium phosphate ceramics used in this study: **(A)** calcium hydroxylapatite, **(B)** beta tricalcium phosphate, and **(C)** biphasic calcium phosphates consisting of 40/60 (β-TCP/HA).

(Calcitite) implant at the interface between the implant and the new bone [1, 12, 13].

The aims of this study were to determine the mechanism for the formation of the new crystals associated with the HA ceramic implants, and to determine the effect at the crystal level (if any) of the following factors: sites of implantation (osseous/nonosseous), time of implantation (2 weeks to 12 months), type of Ca-P ceramic implants (HA, β-TCP, BCP), and experimental subjects for implantation (mice, rabbits, dogs, humans). To determine the mechanism at the crystal level, high resolution transmission electron microscopy (Hr TEM) combined with electron nanodiffraction (diagram obtained from area of less than 10 nm in diameter) and electron probe microanalysis were used on undecalcified sections.

Materials and Methods

The Ca-P ceramics used were prepared as previously described [14, 15] and characterized by X-ray diffraction (Fig. 1) as HA [$Ca_{10}(PO_4)_6(OH)_2$]; β-TCP [$Ca_3(PO_4)_2$]; and BCP, consisting of 40/60 (weight ratio) mixture of β-TCP and HA. The implants were prepared from pressed powder (12,000 ψ) Ca-P ceramics, sintered at 1,000°C, into 2 × 3 mm blocks.

Implantation Procedures

Subcutaneous implantation site: Blocks were introduced using a trocard 70 under abdominal connective tissues of 13 rabbits, 4 rats, and 6 mice for 3 weeks to 3 months.

Osseous implantation site: One hundred eighteen blocks were implanted in calibrated drilling hole of lamellar femoral cortical bone without bone marrow, of cancellous vertebral bone, of cortical alveolar bone, and mastoidal bone of 20 beagle dogs for 3 to 12 months. Ten human periodontal pockets were filled with HA or β-TCP ceramics in particulate form (0.5–1 mm in diameter), and limited control biopsies of some particulates were recovered with surgical needles after 2 and after 12 months.

TEM Analysis

The calcium phosphate ceramic blocks retrieved after implantation and blocks that were not implanted were fixed in a 2% glutaraldehyde solution in cacodylate buffer, pH 7.4, for 2 hours and postfixed for 1 hour in osmium tetraoxide acid in the same buffer. The fixed specimens were embedded in a mixture of methyl-butylmetacrylate (50/50 by volume). Undecalcified ultrathin sections were obtained using a diamond knife on a Sorval Porter ultramicrotome. The sections were contrasted in lead citrate and uranyl acetate and examined with Hr TEM in TEM-SCAN Jeol 200 CX, operating at 200 kV. Electron micromicrodiffractions were performed with an ASID attachment on areas less than 10 nm in diameter; microanalyses were made with dispersive energy electron microprobe EDAX 9100/60 from the same area. Horizontal detector was used with tilt and takeoff angle of 45 and 24%, respectively and resolution of 158ev. Crystallographic interpretation of the HA or β-TCP lattice patterns obtained in Hr TEM were made based on the stereographic projection of the main apatite lattice planes, using a Wulff net to locate the spots of the principal planes on the projections, according to the methods previously described [16, 17].

Microporosity measurements were performed on TEM micrographs using a digitalizer table associated with an IBM AT2 computer.

Infrared absorption spectroscopic analysis of materials before and after implantation were made on Perkin-Elmer 983 G spectrometer on samples pressed into pellets (1 mg sample/300 mg KBr, IR grade, 12,000 ψ). Identification of absorption bands were made according to earlier studies [18].

Results

Changes in Macroproperties of Ceramic Before and After Implantation

Hr TEM of Ca-P ceramic materials (HA, β-TCP, or BCP) before implantation showed them to consist of spherical crystals, 0.1–0.2 μm in diameter, connected together at grain boundaries with micro-

porosity of <10 μm between particles (crystal aggregates).

The number of crystals per unit area is directly related to the microporosity (spaces between the particles in the ceramics); crystal dissolution increases the microporosity. Microporosities were calculated as the ratio of the area covered by the spaces to the area covered by the ceramic particle. The differences in microporosities before and after implantation (3 months in osseous sites in dogs), demonstrated the dissolution of some HA crystals, and more extensively the β-TCP crystals as demonstrated by BCP microporosity increase. The relation between increase in microporosity and the β-TCP content in BCP ceramics with various HA/β-TCP ratio was described in a previous work of the authors [9].

Observations on Implant Surface After Implantation

In both osseous and nonosseous sites, tissue integration with subsequent formation of collagen fibers at the implant surface and peripheries as observed. After 2 months in rabbits, implants from nonosseous sites showed that the surrounding collagenous network remained unmineralized and showed clusters of needle-like microcrystals (new crystals) in the immediate vicinity of the aggregates of large crystals of the ceramic implant (Fig. 2a). In marked contrast, the collagenous network surrounding the ceramic implanted in osseous sites of the same animal was densely mineralized with needle-like microcrystals (Fig. 2b). The same results were obtained in rats, mice, and dogs.

Implants recorded from osseous sites in dogs after 9 months showed the presence of well-mineralized bone in contact with the implant surface (Fig. 3), whereas implants from nonosseous sites in the same animal showed no bone formation, only the presence of new crystals associated with the ceramic crystals.

Observations in Microporous Regions Below Surface (0–20 μm)

A greater abundance of the new crystals was observed between ceramic crystals in implants recovered from osseous sites after 2 months (Fig. 2b, arrows in the same rabbit, compared to the population of these crystals in implants from nonosseous sites in dogs even after 4 months, Fig. 4). The filling of microporosity by biological apatite microcrystals was very significant after 2 months in osseous sites (Fig. 2b), whereas the microporosities were only sparsely filled in nonosseous sites (Fig. 4).

The crystals in the new bone surrounding the implants in human bone were parallel in shape, with a thickness of 2–5 nm (Fig. 5). Observations were similar in osseous sites in animals. Differences in the density of the new crystals was observed among the surface, the sub-surface, and the body of the implants recovered from both osseous and nonosseous sites in rabbits (Fig. 6). The new crystals were always associated with the much larger ceramic crystals in the body of the implant, and its formation appeared not to be related to implantation sites, type of Ca-P ceramics, duration of implantation, and subject of implantation. The only difference observed was the abundance or density of the new crystals, i.e., more new crystals were observed in implants from osseous than from nonosseous sites. At higher magnification, the intimate association of the new crystals with the larger ceramic crystals is more evident (Fig. 7). The new crystals found in the micropores of the ceramics were acicular in shape compared to the parallel shape of the bone crystals from the new bone and from the host bone (Fig. 5). In dogs after 4 months, all the spaces in the microporous regions have been filled with the new crystals and no further change was observed in dogs (Fig. 8) or in human even after 12 months.

Relationship of New Crystals with Ceramic Crystals

The formation of the new microcrystals between

Fig. 2. TEM of dense β-TCP implants in rabbit recovered after 8 weeks. (**a**) Implant in abdominal connective tissue showing the presence of nonmineralized collagenous matrix at the surface of the β-TCP ceramic. (**b**) Implant in femoral cortical bone showing the mineralization process of the peripheric osteoid matrix on the β-TCP ceramic surface implanted in rabbit cortical femoral bone. ×20,000.

Fig. 3. TEM showing bone mineralized collagenous matrix coalescing with the surface of BCP implant (arrow in cortical mastoidal dog bone after 9 months. ×15,000.

Fig. 4. TEM of dense HA implant on dog connective tissue during 4 months showing needle-like crystals (arrow) filling the spaces (microporosity) between the ceramic crystals (C). ×40,000.

Fig. 5. TEM of cross-section of crystallites in sound human periodontal bone showing the width (w) and thickness (t). ×100,000.

Fig. 6. TEM of dense HA granules after 4 months implantation in human periodontal pockets. Ultrathin section from the implant surface (S) to the depth (d). ×5,000.

Fig. 7. Higher magnification of Figure 6 showing new crystals (arrow) on the surface and between the ceramic crystals (C). ×100,000.

Fig. 8. New crystals inside the microporosity of a BCP ceramic after 1 year implantation in cortical mastoidal bone of dog. ×50,000.

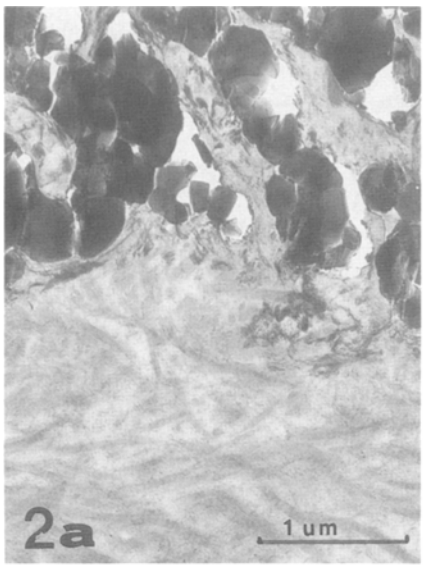
2a
1 um


2b
1 um

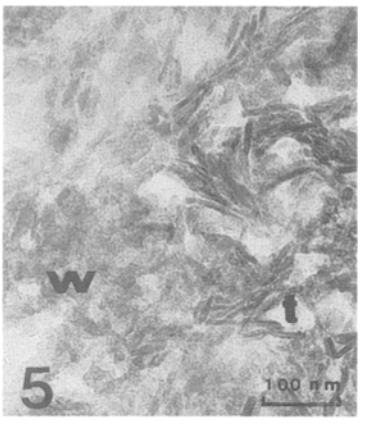
w
t
5
100 nm


3
1 um

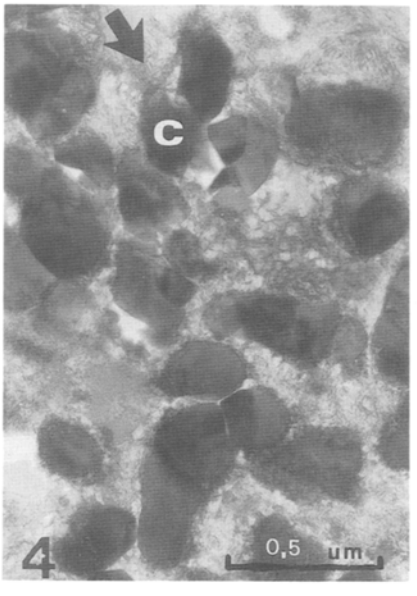
c
4
0,5 um

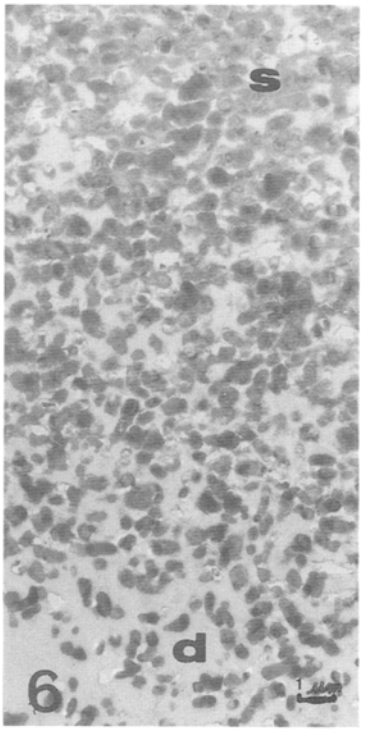
s
d
6

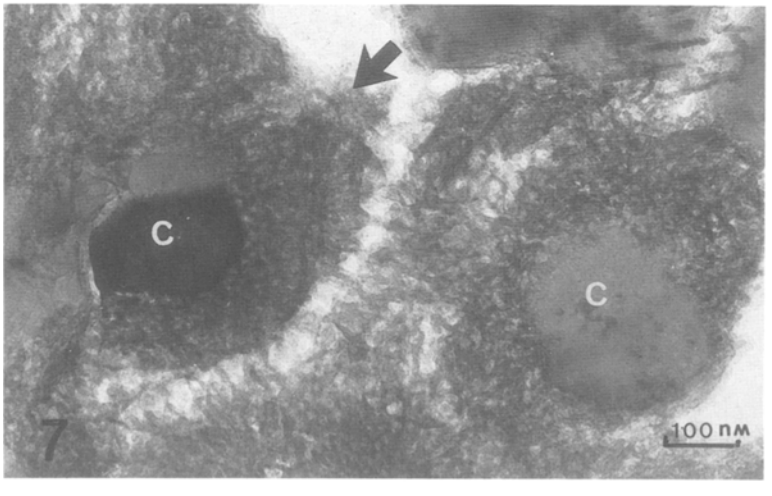
c
c
7
100 nm

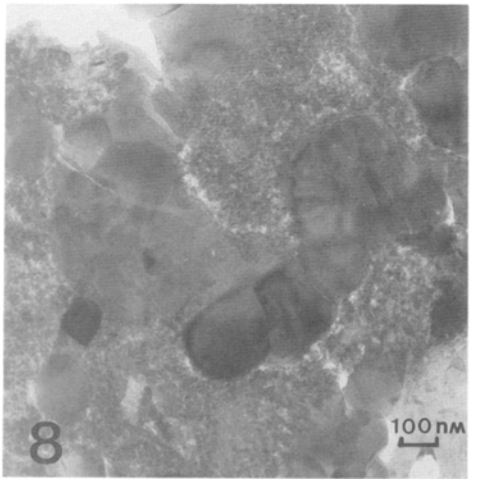
8
100 nm

and on the surface of the ceramic particles was observed after 3 weeks in mice (Fig. 9) and appeared perpendicular to the ceramic crystal surface like the spine of the sea urchin.

In order to study the relationship between the new crystals and the Ca-P ceramic crystals, Hr TEM analyses at the lattice plane level were performed. The new microcrystals associated with the surface of individual HA ceramic crystal had their c-axes parallel to each other (Fig. 10). Hr TEM of the junction of the new crystals and the ceramic HA crystals revealed apatitic lattice plane of 0.82 nm, corresponding to the (100) apatite lattice plane (Fig. 11). Electron micro-microdiffraction of this area (less than 10 nm in diameter) gave rings of 0.345 and 0.82 nm, respectively, corresponding to the apatite planes (Fig. 12). Electron probe microanalyses of these crystals gave a Ca/P weight ratio of 2.4, similar to the value obtained from neighboring bone apatite crystals, and higher than the Ca/P value (2.2) obtained from the HA crystals of the ceramic implants.

The new microcrystals associated with the much larger β-TCP and HA crystals of the ceramics were similarly identified as being apatitic. The Hr TEM of the new crystals located on the surface of both HA or β-TCP crystal ceramics gave rings of 0.53 and 0.82 nm corresponding to the apatite (101) and (100) lattice planes, respectively, and a measured angle of 72° corresponding to the calculated angle of 71.2° in synthetic HA (Fig. 13). Only one family of lattice planes of the new crystals was found in continuity with the lattice planes of the single crystals of the HA ceramic material, or more important, on β-TCP crystal ceramic (Fig. 14).

Linear defects (edge dislocations) and flexions were also observed at the biological apatite/ceramic crystal junction caused by the differences in the reticular distances of biological apatites and β-TCP crystals (Fig. 14).

Infrared absorption spectra of the ceramic implant before and after implantation in bony sites showed that the new material is different from the HA ceramic material by the presence of CO_3^{2-} substituting in the apatite lattice (Fig. 15) similar to that observed with implants from nonosseous sites [11].

Hr TEM studies demonstrated the increase in the microporosities after implantation of all Ca-P ceramics. These results indicated a dissolution process at the crystal level. Simultaneously, the precipitation of apatitic crystals was observed.

Results of this study are briefly summarized as follows: (1) increase in microporosity after implantation and simultaneous appearance of needle-like crystals closely associated with the much larger crystals of the Ca-P ceramic implants (Figs. 3, 4, 6, 7, 8); (2) continuity in the lattice planes of the new apatite crystals with the lattice planes of the HA or β-TCP crystals in the Ca-P ceramic implant; (3) the new crystals were identified as apatitic by electron micro-microdiffraction techniques (Fig. 12) and as a CO_3 substituted apatite by infrared analyses (Fig. 15), similar to bone apatite crystals; (4) the formation of these new crystals was unrelated to implantation site, type of Ca-P ceramics, duration, and subject species (Figs. 2, 4, 7, 9); (5) the differences in features between implants from osseous and nonosseous sites were greater abundance of the new crystals in implants from osseous sites (Figs. 2, 3, 4, 7, 8), absence of mineralized collagen in implants from nonosseous sites (Fig. 2), and absence of "true bone" formation in nonosseous sites.

Discussion

The main attractive feature of the Ca-P ceramic and bioactive glass ceramics is their ability to form a strong bond with the host bone compared with other inert ceramics (e.g., alumina) or metal implants [1, 2, 12, 19, 20, 21–23]. The strong bond associated with HA ceramics has been attributed to a "bonding zone" described as electron dense "amorphous" material. TEM of undecalcified sections from the bone-HA interface showed the presence of microcrystals described as biological apatite, deposited perpendicular to the HA ceramic surface and associated with collagen fibers [1, 12].

Fig. 9. TEM of β-TCP ceramic after 21 days subcutaneous implantation in mice. Acicular crystals (arrow) can be observed at the surface of ceramic crystals (g). ×30,000.

Fig. 10. TEM of dense HAP particles after 2 months implantation in human periodontal pocket, showing crystallites (arrow) forming perpendicular to the ceramic crystal surface. ×150,000.

Fig. 11. Higher magnification of the crystallites in Figure 10. ×730,000.

Fig. 12. Micro-microdiffraction of the crystallites in Figure 11.

Fig. 13. Higher magnification of crystallites associated with the HA ceramic crystal showing the lattice plane (100) and (101) of apatite. ×1,350,000.

Fig. 14. Epitaxial growth of the new apatite crystals (arrow) on β-TCP ceramic crystals after 15 days implantation in connective tissue. Linear defect can be observed at the interface (light arrow). ×1,350,000.

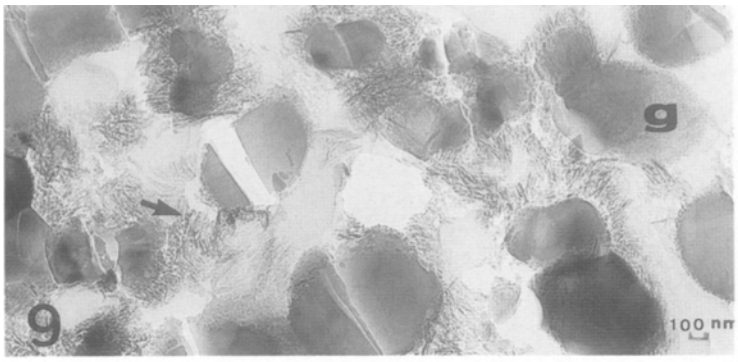
g
9
100 nm


10
100 nm

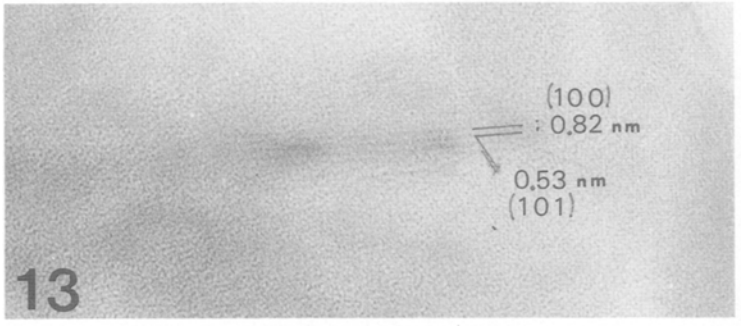
(100)
0.82 nm
0.53 nm
(101)
13

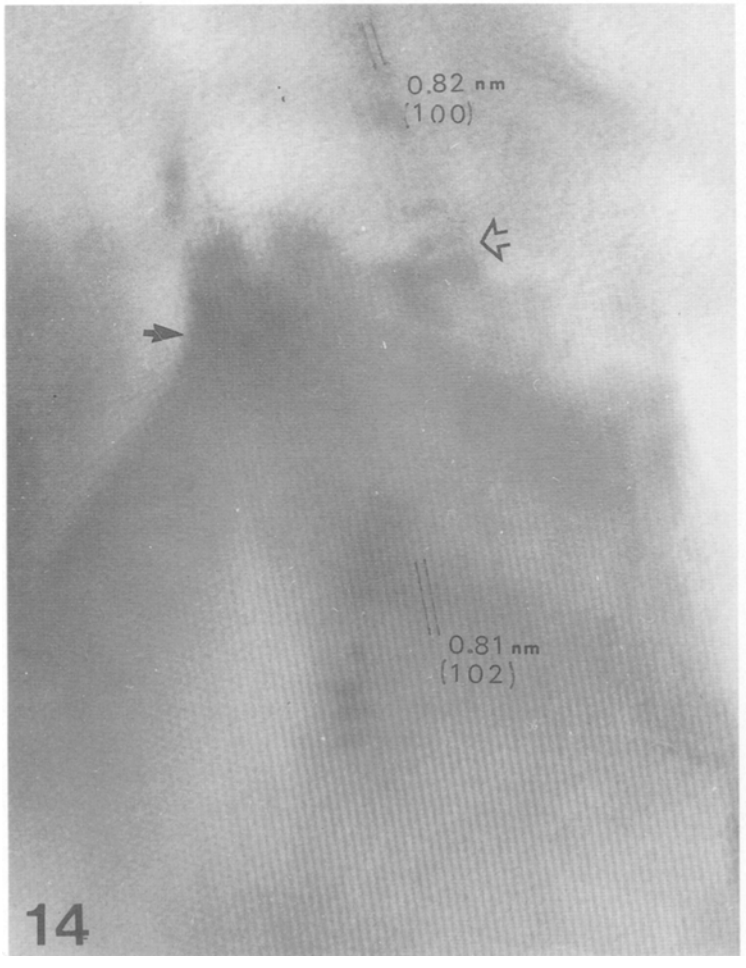
0.82 nm
(100)
0.81 nm
(102)
14

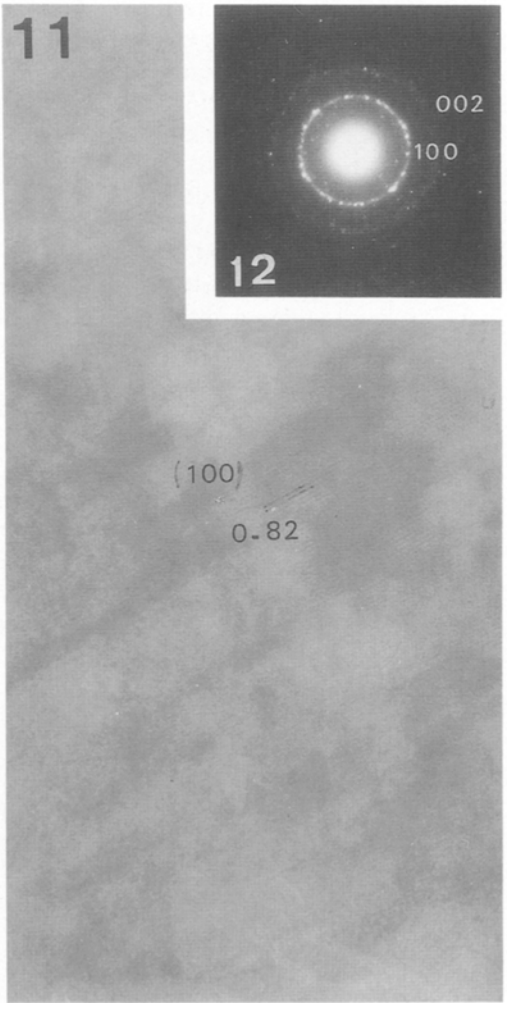
11
(100)
0-82

002
100
12

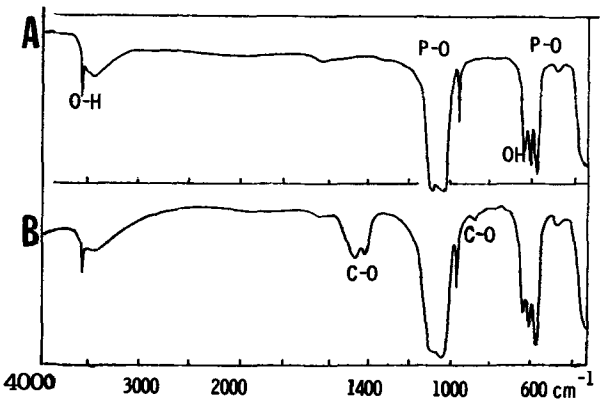

Fig. 15. Infrared transmission spectra of HA before (A) and after (B) implantation. The biological apatites associated with the ceramics differ from the material before implantation in being less crystallized (lower resolution of absorption bands) and in having CO_3-substituted in the apatite [18].

The results of the present study extended the observations reported previously [12, 21], i.e., that the "bonding zone" at the bone-ceramic implant interface consists of an area of mineralized matrix in osseous site of implantation. The use of Hr TEM in this study demonstrated *for the first time, the nonspecific formation of new crystals* (i.e., not related to implantation site, subjects of implantation, and types of ceramics) in the subsurface and in the core of the Ca-P ceramics after implantation. The new crystals were not necessarily deposited on collagenous fibers and demonstrated some specific crystallographic interactions with the HA or -TCP crystals of the ceramic. Contrary to the observations reported by Tracy and Doremus [13], the shape of the new crystals were observed to be different from those of the bone crystals, i.e., acicular vs. parallel-shaped.

The apatitic microcrystals in the micropores regions were shown similar to biological apatites in terms of containing carbonate as a substituent in the apatite [18]. These biological apatites associated with Ca-P ceramics were similar in spectral properties to those observed associated with HA ceramics implanted in nonosseous sites [11] and those suspended in serum *in vitro* [24]. The new crystals were also similar to the bone apatite crystal in terms of Ca-P weight ratio as shown by electron probe microanalysis.

Hr TEM studies demonstrated the increase in microporosity after implantation indicating the dissolution of some HA and/or β-TCP ceramic crystals (Table 1), confirming earlier reports that after the first weeks of implantation, the Ca-P ceramics in osseous and nonosseous site of implantation appeared to have undergone partial bioresorption by intra- and extracellular activity [2, 3, 25–30].

It is reasonable to assume that the formation of the carbonate apatite crystals would slow down further dissolution of the implant by reducing the spaces available for fluid diffusion which would cause the separation of the individual crystals from the ceramic particle.

The observed formation of carbonated apatites within the micropores of the Ca-P ceramics regardless of implant sites, osseous or nonosseous, indicated a process of calcification without cell differentiation. However, the histological properties of true bone formation was observed only in osseous sites, confirming the present general agreement of the scientific community regarding the nonosteogenic properties of the Ca-P ceramics [25, 35]. It appeared that the Ca-P ceramics were able to promote calcification in both osseous and nonosseous sites but not to induce true osteogenesis in nonosseous sites.

The formation of the CO_3-apatite after implantation of the Ca-P ceramics (HA, β-TCP, or BCP) in osseous or nonosseous sites [8–11] (and this study) or after suspension in cell culture [24, 31] or in serum [31, 32] could result from either or both of the following processes (Fig. 16): (1) partial dissolution of the HA or β-TCP crystals of the ceramic causing an increase in the supersaturation level of the immediate microenvironment of the implant, subsequently leading to the precipitation of the new apatite crystals incorporating other ions (e.g., CO_3^{2-} from the biological fluid during its formation), and/or (2) precipitation of the new apatite crystals with or without the dissolution of the ceramic crystals, the ceramic particles acting as nucleator or seeds (Figs. 9, 10, 14).

Renooij et al. [32], using labeled β-TCP implant with Sr^{85}, suggested that the β-TCP may have been transformed into apatite in the physiological environment [33]. Our Hr TEM study *demonstrated the epitaxial growth* of the new crystal on the surface *of either HA or β-TCP crystal of the ceramic* (Figs. 10, 14). The lattice pattern distortions observed at the junction of the new apatite and β-TCP crystal (Fig. 14) also corroborates the epitactic crystal growth process.

In conclusion, the results from this study indicate that all the noncommercial Ca-P ceramics tested biodegrade, causing the formation of carbonate-substituted apatites which become incorporated in the new bone in osseous sites. The formation of similar apatites associated with Ca-P ceramics implanted in nonosseous sites is not due to any osteo-

genic properties of the material but to dissolution/reprecipitation and/or epitactic seeded growth processes.

Acknowledgments. The helpful discussions with Prof. B. Kerebel are gratefully acknowledged. This work was supported by INSERM Reseau de Recherche Clinique (Director, Prof. B. Kerebel) and in part by the National Institutes of Health Research Grant Nos. DE-04123 and DE-07223 (R. Z. LeGeros).

References

1. Jarcho M (1981) Calcium phosphate ceramics as hard tissue prosthetics. Clin Orthop 157:259–278
2. De Groot K (1983) Bioceramics of calcium phosphate. CRC Press, Boca Raton, Florida
3. Metsger DS, Driskell TD, Paulstrud JR (1982) Calcium phosphate ceramic, a resorbable bone implant: review and current status. J Am Dent Assoc 105:1035–1038
4. Van Reamdonck W, Ducheyne P, De Meester P (1984) Calcium phosphate ceramics. In: Ducheyne P, Hastings G (eds) Metals and ceramic biomaterials. CRC Press, Boca Raton, Florida, pp 144–166
5. LeGeros RZ (1988) Calcium phosphate materials in restorative dentistry: a review. Adv Dent Res 2:164–180
6. Nery EB, Lynch KL (1978) Preliminary clinical studies of bioceramic in periodontal osseous defects. J Periodont 49:523–527
7. Daculsi G (1988) Biological properties of calcium phosphate biomaterials. In: Babighian G, Veldman JE, Portmann M, Zini C (eds) Transplants and implants in otology. Kugler and Ghedini Publications, Amsterdam, 227–230
8. Daculsi G, LeGeos RZ, Heughebaert M, Jans I (1988) Biological apatites associated with calcium phosphate ceramics implanted in osseous and non-osseous sites. J Dent Res 67:370
9. Daculsi G, LeGeros RZ, Nery E, Lynch K, Kerebel B (in press) Transformation of biphasic calcium phosphate ceramics in vivo. Ultrastructural and physico-chemical characterization. J Biomed Mat Res
10. Frank RM, Gineste M, Benque EP, Hemmerle J, Duffort JF, Heughebaert M (1987) Etude ultrastructurale de l'induction osseuse apres implantation de bioapatities chez l'homme. J Biol Buccale 15:125–134
11. Heughebaert M, LeGeros RZ, Gineste M, Guilhem A (1988) Hydroxyapatite (HA) ceramics implanted in non-bone-forming sites. Physico-chemical characterization. J Biomed Mat Res 22:257–268.
12. Jarcho M, Kay JF, Drobeck HP, Doremus RH (1976) Tissue, cellular and subcellular events at bone-ceramic hydroxylapatite interface. J Bioeng 1:79–92
13. Tracy BM, Doremus RH (1984) Direct electron microscopy studies of the bone hydroxylapatite interface. J Biomed Mater Res 18:719–726
14. Heughebaert M, Daculsi G, Heughebaert JC, D'Yvoire F (1986) Calcium aluminum phosphate for biological applications. In: Christel P, Meunier A, Lee AJC (eds) Biological and biomechanical performance of biomaterials. Elsevier Science Publishers, BV, Amsterdam, pp 33–38
15. LeGeros RZ (1986) Variability of β-TCP/HA ratios in sintered "apatites." J Dent Res 65:292
16. Daculsi G, Kerebel B, Verbaere A (1978) Methode de mesure des cristaux d'apatite de la dentine humaine en microscopie electronique de haute resolution. C R Acad Sci Paris 286:1439–1441
17. Kerebel B, Daculsi G, Verbaere A (1976) Ultrastructural and crystallographic study of biological apatites. J Ultrastruct Res 57:266–275
18. LeGeros RZ, LeGeros JP, Trautz OR, Klein E (1970) Spectral properties of carbonate in carbonate containing apatites. Dev Appl Spec 7B:3–12
19. Osborn JF, Newesely H (1980) The material science of calcium phosphate ceramic. Biomaterials 1:108–111
20. Ducheyne P (1987) Bioceramics: material characteristic versus in vivo behavior. J Biomed Mater Res 21:219–236
21. Ganeles J, Listgarten MA, Evian CI (1986) Ultrastructure of durapatite periodontal tissue interface in human intrabony defects. J Periodontol 57:133–140
22. Hench LL, Splinter RJ, Allen WC, Greenlee TK (1971) Bonding mechanisms at the interface of ceramic prosthetic materials. J Biomed Mater Res 2:117–141
23. Gross U, Schumacher D, Strunz V (1983) Comparative studies on the tissue reaction after implantation of glass ceramic into human, pig, rat, chicken bones. In: Vincenzine P (ed) Ceramics in surgery. pp 161–168
24. Gregoire M, Orly I, Kerebel LM, Kerebel B (1987) In vitro effects of calcium phosphate biomaterials on fibroblastic cell behavior. Cell Biol 59:255–260
25. LeGeros RZ, Parsons R, Daculsi G, Diressens F, Lee D, Metsger S (1988) Biodegradation/bioresorption of calcium phosphate ceramics: task group report. In: Ducheyne P, Lemons J (eds) Bioceramics: material characterization vs. in vivo behavior. Ann NY Acad Sci 523:268–291
26. Cameron HU, Macnab I, Pilliar RM (1977) Evaluation of a biodegradable ceramic implant. J Biomed Mater Res 11:179–181
27. Daculsi G, Orly I, Gregoire M, Heughebaert M, Hartmann DJ, Kerebel B (1986) Cell interactions with mixed calcium phosphate (TCP and HA) and alumina solid phase: an ultrastructural study. In: Advances in biomaterials: biological and biomechanical performances of biomaterials, vol IV. ESV Publishers, Amsterdam, pp 337–342.
28. Daculsi G, Hartmann DJ, Heughebaert M, Hamel L, Le Nihouannen JC (1988) In vivo cell interactions with calcium phosphate. J Submicroscop Cytol 20:379–384
29. Klein CPAT, Driessen AA, De Groot K (1984) Relationship between the degradation behavior of calcium phosphate ceramics and their physical chemical characteristics and ultrastructural geometry. Biomaterials 5:157–160
30. Osborn JF, Donath K (1984) Die ensale implantation von hydroxylapatite keramik und tricalciumphosphatkeramik: integration vs substitution. Deutsch Zahn Zeit 39:970–976
31. LeGeros RZ, Orly I, Gregoire M, Abergas T, Kazimiroff J (1987) Physico-chemical properties of calcium phosphate biomaterials used as bone substitutes. Trans 13th Ann Meeting Biomaterials (abstract 84)
32. Renooij W, Hoogendoorn A, Visser WJ, Lentferink RHF, Lentferink MGJ, Van Leperen H, Oldenburg SJ, Janssen WM, Akkermans LMA, Wittebol P (1985) Bioresorption of ceramic strontium 85-labeled calcium phosphate implants in dog femora. A pilot study to quantitate bioresorption of ceramic implants of hydroxylapatite and tricalcium orthophosphate in vivo. Clin Orthop Rel Res 197:272–285
33. Amler MH (1987) Osteogenic potential of non-vital tissues and synthetic implant materials. J Periodont 58:758–761

Received February 24, 1988, and in revised form March 31, 1989.